

The Effect of Slip Velocity on Saturation for Multiphase Condensing Mixtures in a PEM Fuel Cell

Mohammad J. Kermani¹

Department of Mechanical Engineering
Amirkabir University of Technology (Tehran Polytechnic)
Tehran, Iran, 15875-4413

John M. Stockie

Department of Mathematics
Simon Fraser University
Burnaby, British Columbia, Canada, V5A 1S6

Abstract

In this paper, we have developed an approximate formula for liquid saturation within a two phase condensing mixture that relates the saturation level to the slip velocity between the gas and liquid phases. In particular, we have explained why models in which the slip velocity is assumed to be zero exhibit a saturation that is several orders of magnitude smaller than in other models where slip velocity was allowed to vary. This is a discrepancy that has appeared in computed results reported in the fuel cell literature, but which has not yet received a satisfactory explanation. We demonstrate that the reason behind the large discrepancy is rooted in the type of model used to treat the slip velocity between phases.

Keywords: Condensation – Two Phase Flow – PEM Fuel Cell – Slip Velocity

¹Corresponding Author, E-mail: mkermani@aut.ac.ir, [www: me.aut.ac.ir/mkermani.htm](http://www.me.aut.ac.ir/mkermani.htm)

Nomenclature

A	area
a, b, c	positive constants, Eqn. (2)
C, C'	positive coefficient of order 1; Eqns. (20) and (23)
c_l	liquid specific heat value
c_p	isobar specific heat value
C_s	positive coefficient, Eqn. (6)
d_l	diameter of liquid droplet
h	convective heat transfer coefficient
k	thermal conductivity
L_{fg}	local value for enthalpy of phase change
m	mass
N_u	Nusselt number
P_r	Prandtl number
\dot{Q}	heat transfer rate
Re	Reynolds number
S	saturation
t	time
T	temperature
V	velocity
x	spatial dimension

Greek symbols

α	vapor phase volume fraction
ρ	density
Ψ	condensation/evaporation parameter, Eqn. (12)
μ	dynamic viscosity

Subscripts

l	liquid phase
v	vapor phase
s	slip velocity

1 Introduction

In this paper, we investigate the dependence of liquid saturation on slip velocity within a two-phase condensing mixture. In gas-liquid mixtures in which water is the only condensing component, the liquid saturation is the ratio of the volume fraction of liquid water to that of the total water (liquid water + water vapor) and is denoted by S . The slip velocity, V_s , is the relative velocity between the water vapor and liquid water phases. We focus on an application to multiphase flow in the cathode of a proton exchange membrane fuel cell (or PEMFC) for which the condensing gas mixture is typically composed of oxygen, nitrogen and water.

Within the literature on multiphase condensing mixtures, and fuel cells in particular, models may be separated broadly into two classes: *mist models* in which the liquid is assumed to move at the same velocity of the gas (that is, $V_s = 0$); and true *multiphase flow models* wherein the liquid moves at a velocity that is not necessarily the same as the gas velocity, and is determined by physics such as shearing forces, capillary forces, etc. (so that $V_s > 0$). Under normal fuel cell operating conditions, these two classes of model lead to very different values of saturation, which can differ by up to several orders of magnitude! To the best of our knowledge, no explanation for this discrepancy has appeared in the literature, and certainly not in any discussion of fuel cell models. The present paper aims to fill this gap. Prior to computing problems of this type, an order of magnitude analysis is required to determine the size of the droplet (or liquid pocket), and we conclude that when droplets are above a micron in size, the mist model should be avoided.

A review of various PEMFC models that include liquid water effects is provided by Weber and Newman [25]. Among the authors that employ a mist model (for example, [5, 8, 13, 20, 22, 23]), many depict only the regions in a fuel cell in which condensation is occurring rather than the quantity of condensed liquid water; those authors that do report saturation levels for mist model computations obtain values of S below 0.01% by volume. By contrast, multiphase flow models such as [3, 4, 9, 19, 24, 15, 16] report values of S that lie mostly between 5% and 30%, but may be as large as 100% in the case of [19].

Our main aim in this paper is to identify the source of this discrepancy in saturation results, which we attribute to an assumption on the slip velocity that drives the liquid droplets in the gas phase. As the liquid droplet/pocket sizes increase, their inertia also increases and this causes a lag in the response of the liquid phase to the corresponding driving force. Therefore, there should be a strong connection between the droplet sizes and the slip velocity between the phases.

In this paper, a single component (pure) steam flow undergoing condensation process is studied. The extension to a multicomponent condensing mixtures is straightforward. By writing down an energy balance for a given volume of liquid water undergoing condensation, we demonstrate that saturation S increases with the slip velocity between phases (see Eqn. 15). We then employ an order of magnitude analysis to develop a relationship between saturation and slip velocity (see Eqn. 24), which is then supported with computational results taken from literature. The extension to a multicomponent gas mixture is straightforward and so only the single component case is treated in this work.

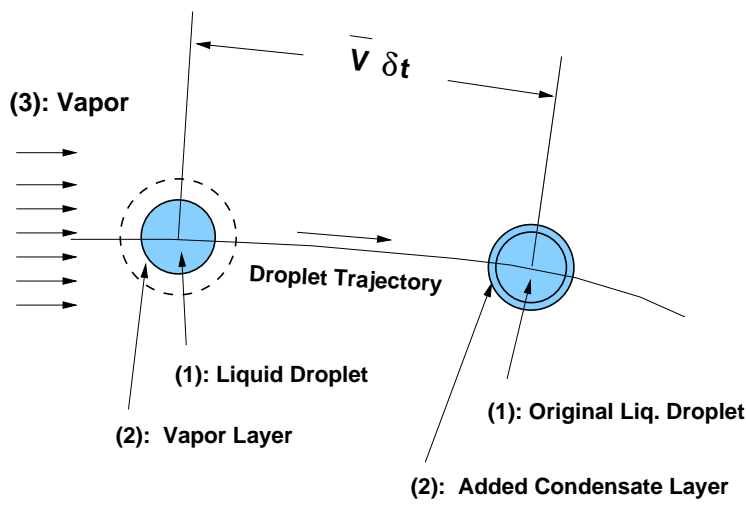


Figure 1: Schematic of a liquid droplet, growing by condensation along its trajectory within the time step δt .

2 The Relationship Between Saturation and Slip Velocity

2.1 Theoretical Development

For a condensing two-phase flow mixture, we develop an equation relating the condensation rate to the slip velocity between phases. There is a long list of parameters that might affect the condensation rate, but we focus here on the most relevant ones. Some of these parameters are: droplet size, duct length scale (how spacious is the duct cross section), liquid/gas phase exposure time, etc. The droplet sizes (or in general the size of any liquid pocket) and the slip velocity are parameters that are strongly dependent on each other. Small droplets/liquid pockets (if they are sub-micron in size) follow the gas phase with the same velocity [1, 2] (i.e. zero slip velocity between the phases). Because the liquid particles are very small, they possess very minor mass inertia. Hence, they behave as mist or fog suspended within a carrier gas flow.

On the other hand, if the droplets are above one micron in size, they will possess greater inertia and can lag behind the carrying gas. Hence, a slip velocity between the phases is required. In other words, neglecting the slip velocity in a two-phase flow is equivalent to assuming that the droplet size should be small (sub-micron). Although the duct opening size and exposure time of the liquid and gas phases are important parameters, the slip velocity is of primary importance in determining saturation levels for the type of two-phase flows considered here.

We now develop an equation relating the steam condensation rate to the slip velocity between the liquid water and water vapor. To do so, we consider a single liquid water droplet of mass m_ℓ , temperature T_ℓ , and specific heat c_ℓ , which is moving with velocity \vec{V}_ℓ along the trajectory shown in Fig. 1. The droplet is surrounded by water vapor having a temperature T_v , and both phases are embedded within a medium that has convective heat transfer coefficient h . In the case of transport in a fuel cell cathode, the gas is typically a multicomponent mixture consisting of oxygen, nitrogen and water vapor; however, extending our argument to deal with a multicomponent gas is straightforward and so we consider water vapor only.

The heat transfer coefficient h is determined from the Nusselt number Nu (specified at the

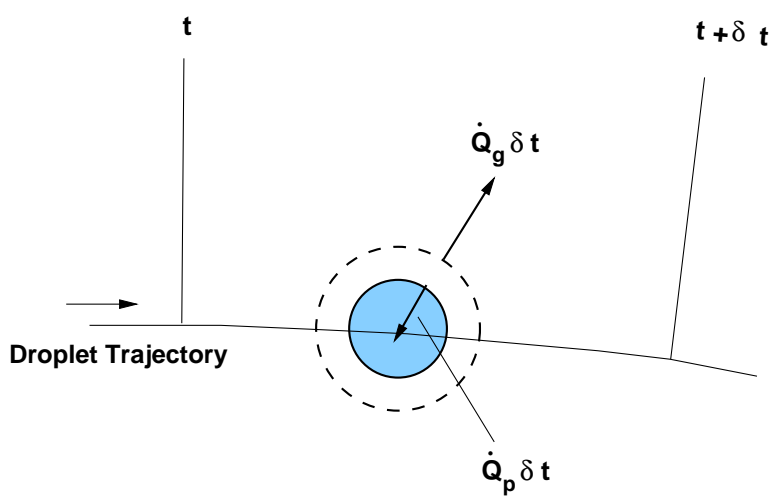


Figure 2: A representation of the latent heat released in a condensation process, which is absorbed into the liquid droplet and by the surrounding vapor.

surrounding flow conditions) according to

$$h = \frac{Nu \kappa_v}{d_\ell}, \quad (1)$$

where κ_v is the thermal conductivity of the gas and d_ℓ is the liquid droplet diameter. Assuming that the fluid can be treated as a continuum, any dependence of the Nu on the Knudson number can be ignored and therefore Nu can be written in terms of the Reynolds and Prandtl numbers as

$$Nu = a Re_v^b Pr_v^c, \quad (2)$$

where a , b , and c are known positive constants that depend on flow conditions and geometry (see [11], for example). In Eqn. 2 Re_v and Pr_v are, respectively, the Reynolds and Prandtl numbers obtained at either the gas temperature or the average temperature of the gas and liquid:

$$Re_v = \frac{\rho_v V_s d_\ell}{\mu_v}, \quad (3)$$

$$Pr_v = \frac{\mu_v c_{p_v}}{\kappa_v}. \quad (4)$$

Here, we denote by ρ_v the density, μ_v the dynamic viscosity, and c_{p_v} the iso-bar specific heat, where the subscript “ v ” refers to the gas (vapor) phase. The slip velocity can be written as $V_s = V_v - V_\ell$, where V_v is the velocity of the gas and V_ℓ is that of the liquid droplet. Finally, we note that Eqn. 2 is a general result that applies to both laminar and turbulent conditions.

We next substitute Eqns. 2, 3 and 4 into Eqn. 1 to obtain a relationship between the convective heat transfer coefficient and the slip velocity

$$h = C_s (V_s)^b, \quad (5)$$

where C_s is a positive coefficient given by

$$C_s = a \left(\frac{\rho_v d_\ell}{\mu_v} \right)^b Pr_v^c.$$

It is therefore possible to conclude the following:

Conclusion 1 *The heat transfer coefficient h is an increasing function of the slip velocity V_s ; that is, $\partial h / \partial V_s > 0$.*

Next, we consider the effect of the heat transfer coefficient on saturation. Consider again Fig. 1, which divides the region of interest into three subregions labeled 1, 2 and 3. Region 1 is at the core of the liquid droplet at time t and remains liquid throughout the trajectory. Region 3 consists of vapor at time t and remains so until time $t + \delta t$. Finally, Region 2 begins as a vapor layer surrounding the core liquid at time t , and is converted to liquid after a time δt owing to condensation. We consider an energy balance for this condensing layer, and recognize that the latent heat contained within Region 2 must transfer either outward (into the gas) or inward (into the liquid droplet) as shown in Fig. 2. This process is represented by the following energy balance

$$(L_{fg}) \frac{dm_\ell}{dt} = \dot{Q}_v + \dot{Q}_\ell, \quad (6)$$

wherein (L_{fg}) is the local value of latent heat. The quantity \dot{Q}_v is the portion of latent heat that flows toward the vapor, and is given by

$$\dot{Q}_v = h A_\ell (T_\ell - T_v), \quad (7)$$

where $A_\ell = \pi d_\ell^2$ is the surface area of the liquid droplet. The second source term in Eqn. 6, \dot{Q}_ℓ , represents the latent heat that moves into the droplet core which is responsible for increasing the droplet temperature

$$\dot{Q}_\ell = m_\ell c_\ell \frac{dT_\ell}{dt}. \quad (8)$$

Substituting Eqns. 7 and 8 into 6, we can rewrite the energy equation for the liquid droplet as

$$(L_{fg}) \frac{dm_\ell}{dt} = h A_\ell (T_\ell - T_v) + m_\ell c_\ell \frac{dT_\ell}{dt}. \quad (9)$$

We can then integrate Eqn. 9 with respect to time over the interval $[t, t + \delta t]$ and obtain

$$\int_{m_\ell(t)}^{m_\ell(t+\delta t)} (L_{fg}) dm_\ell = \int_0^{\delta t} h A_\ell (T_\ell - T_v) dt + \int_{T_\ell(t)}^{T_\ell(t+\delta t)} m_\ell c_\ell dT_\ell.$$

Assuming that all quantities vary only mildly over the infinitesimal time step δt , we can then approximate the integrals above to get

$$(L_{fg}) \Delta m_\ell = h A_\ell (T_\ell - T_v) \delta t + m_\ell c_\ell \Delta T_\ell, \quad (10)$$

where $\Delta m_\ell = m_\ell(t + \delta t) - m_\ell(t)$ is the mass of condensate added and $\Delta T_\ell = T_\ell(t + \delta t) - T_\ell(t)$ is the temperature rise within the liquid over the same time interval.

It was shown in [14] that the latent heat convected away from the condensate layer of Region 2 into the surrounding vapor is much larger than that which is transferred into the liquid (see Figs. 1 and 2); consequently, $h A_\ell (T_\ell - T_v) \delta t \gg m_\ell c_\ell \Delta T_\ell$. This is true for both small droplets (i.e., small m_ℓ) and large droplets in which the term $c_\ell \Delta T_\ell$ is considerably smaller than the latent heat value of (L_{fg}) [1, 2]. We are therefore led to neglect the second term on the right hand side of Eqn. 10. If

we also let $\delta t = \delta x/V_\ell$ (see Fig. 1) and use Eqn. 5 to replace the convective heat transfer coefficient h , then Eqn. 10 can be rewritten as

$$\Delta m_\ell = \frac{C_s (V_v - V_\ell)^b A_\ell (T_\ell - T_v) \delta x}{(L_{fg}) V_\ell}. \quad (11)$$

In this equation, we note that $\Delta m_\ell > 0$ when condensation occurs, and $T_\ell > T_v$ to guarantee the removal of latent heat from the condensate. We can then define the parameter $\Psi \equiv (C_s A_\ell (T_\ell - T_v) \delta x) / (L_{fg})$, so that

$$\Delta m_\ell = \Psi \frac{(V_v - V_\ell)^b}{V_\ell}, \quad (12)$$

where $\Psi > 0$ for condensation.

We can now investigate the effect of changes in V_ℓ on condensation rate Δm_ℓ (or similarly on the saturation). By differentiating Eqn. 12, we obtain

$$\frac{\partial}{\partial V_\ell} (\Delta m_\ell) = -\frac{\Psi}{V_\ell^2} (V_v - V_\ell)^b \left[1 + \frac{bV_\ell}{V_v - V_\ell} \right]. \quad (13)$$

Here, we expect to always have $V_v/V_\ell > 1$ since the gas phase provides a driving force to the motion of liquid, which leads to the following conclusion.

Conclusion 2 *Assuming that $V_v > V_\ell$, the condensation is a decreasing function of liquid droplet velocity; that is, $\partial (\Delta m_\ell) / \partial V_\ell < 0$. Alternatively, we can recast Eqn. 12 in terms of the slip velocity to obtain*

$$\Delta m_\ell = \Psi \frac{V_s^b}{V_v - V_s} \quad (14)$$

so that

$$\frac{\partial}{\partial V_s} (\Delta m_\ell) = \frac{\Psi V_s^b}{(V_v - V_s)^2} \left[1 + \frac{b}{V_s} (V_v - V_s) \right] > 0, \quad (15)$$

which indicates that condensation rate (and consequently also the saturation) is an increasing function of slip velocity. That is, in a model for which the slip velocity between phases is ignored, the condensation rate will be negligible. Alternately, if a model predicts significant saturation levels (say above %20), then the slip velocity between the phases is certainly not zero.

This is the key observation in this paper, and it is supported in the next section by more quantitative arguments that indicate how saturation is affected by various choices of slip velocity.

3 Quantitative Effect of Slip Velocity on Saturation

We begin by writing a mass balance for liquid water

$$\frac{\partial}{\partial t} (\rho_\ell S) + \nabla \cdot (\rho_\ell S V_\ell) = \frac{\dot{m}_\ell}{\mathcal{V}}, \quad (16)$$

where ρ_ℓ is the density of liquid water (defined based on the volume \mathcal{V}_ℓ that the liquid phase occupies), $S = \mathcal{V}_\ell / \mathcal{V}$ is the volume fraction of liquid (or saturation), V_ℓ is the liquid velocity, and

\dot{m}_ℓ/\mathcal{V} is the condensation rate per unit volume. Similarly, mass conservation for the vapor phase can be written as

$$\frac{\partial}{\partial t}(\rho_v \alpha) + \nabla \cdot (\rho_v \alpha V_v) = -\frac{\dot{m}_\ell}{\mathcal{V}}, \quad (17)$$

where ρ_v is the density of the water vapor (defined based on the volume that the vapor phase occupies, \mathcal{V}_v), $\alpha = \mathcal{V}_v/\mathcal{V} = 1 - S$ is the vapor volume fraction, V_v is the vapor velocity, and $-\dot{m}_\ell/\mathcal{V}$ is the evaporation rate per unit volume (which is equal in magnitude but opposite in sign to the condensation rate). By adding together Eqns. 16 and 17, we obtain a conservation equation for the total mass of water (liquid + vapor):

$$\frac{\partial}{\partial t}(\rho_v \alpha + \rho_\ell S) + \nabla \cdot (\rho_v \alpha V_v + \rho_\ell S V_\ell) = 0. \quad (18)$$

In order to evaluate the effect of slip velocity on saturation, we consider in particular the water flux terms from Eqn. 18:

$$\rho_v \alpha V_v + \rho_\ell S V_\ell. \quad (19)$$

We assume that within the condensing regions of a PEMFC electrode, these two terms are of relatively equal importance, and so we write to a first approximation

$$\rho_v \alpha V_v = C \rho_\ell S V_\ell, \quad (20)$$

where C is an $O(1)$ constant. Using this notation, the ratio of gas to liquid volume fraction can be written as

$$\frac{\alpha}{S} = C (\rho_\ell / \rho_v) (V_\ell / V_v). \quad (21)$$

We next compute a concrete value for the volume fraction ratio based on typical PEMFC operating conditions. The density of liquid water is $\rho_\ell \approx 970 \text{ kg/m}^3$ at an operating temperature of $80 \pm 5^\circ\text{C}$. The density of water vapor can be calculated using the ideal gas law as

$$\rho_v = \frac{P_v}{R_v T_v}. \quad (22)$$

Using $R_v = 461 \text{ J/kgK}$ as the gas constant for water vapor, and taking $P_v = P_{sat}(80^\circ\text{C}) = 47400 \text{ Pa}$ as the partial pressure of the vapor (which we assume is equal to the saturation pressure in the two-phase case) we find that $\rho_v \approx 0.290 \text{ kg/m}^3$. For comparison, using thermodynamic tables ρ_v at $T=80^\circ\text{C}$ is found to be 0.293 kg/m^3 [17]. Therefore, the ratio of volume fractions in 21 can be written as

$$\begin{aligned} \frac{\alpha}{S} &\approx 3340 C (V_\ell / V_v), \\ &\approx C' \times 10^4 (V_\ell / V_v), \end{aligned} \quad (23)$$

where C' is an $O(1)$ constant. With $\alpha = 1 - S$,

$$\log_{10} \left(\frac{V_\ell}{V_v} \right) \approx -3.35 - \log_{10} \left(\frac{S}{1-S} \right) \quad (24)$$

Equation 24 is a simple but fruitful expression that relates the ratio of volume fractions to the ratio of velocities for the condensing component of a mixture.

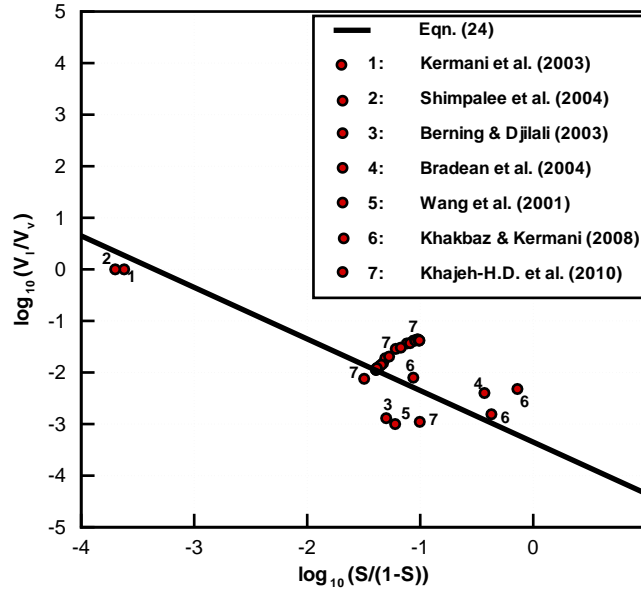


Figure 3: Post-processed data from different references for V_s and S ; and a line-fit to the data: $\log_{10}(V_\ell/V_v) \approx -3.35 - \log_{10}(S/(1-S))$. Note that: $V_\ell/V_v \equiv 1 - V_s/V_v$.

In the case of a mixture having no slip between phases of the condensing component, we clearly have $V_\ell = V_v$ or $V_s = 0$. Consequently, $\alpha = C' \times 10^4 S$. Assuming for the sake of simplicity that $C = 1$, we obtain a saturation of $S = 0.0001$ and so the volume occupied by liquid is negligible. This observation is consistent with the saturation values computed using the mist model by Shimpalee et al. in [22] and Kermani et al. in [13]. A plot of Eqn. 23 is given in Figure 3 on a log-log scale, along with the corresponding data points from these last two sets of computations.

When the slip velocity is non-zero, and in particular when the volumes occupied by liquid and vapor are of approximately equal size, then Eqn. 23 requires that the liquid velocity be approximately four orders of magnitude smaller than the vapor velocity. This is borne out by other computational results reported in the literature using multiphase flow models [3, 4, 24], which lie very close to the straight-line approximation but cluster near the point B in Figure 3.

It is not possible, based on the data available in the literature, to identify specific constraints on flow speed and liquid droplet size for which the mist flow assumption is valid in general. This can be partly attributed to the complexity of two-phase flow, which depends on many parameters like the Weber number (a measure of the tendency of droplets or bubbles to either form or break), Knudsen number, skin friction, Reynolds number, and the second phase parameters.

Nonetheless, it is widely accepted that in certain high-speed two-phase flow applications – such as low pressure steam turbines or vapor nozzles, where V_v can be as high as 400 to 500 m/s and droplet sizes as small as $1 \mu\text{m}$ – the mist flow assumption ($V_s = 0$) can be safely applied [14, 7, 6]. However, for droplets larger than $1 \mu\text{m}$ (in the same speed range) the no-slip assumption between the phases of the condensing component is no longer correct [1, 2]. Another example that demonstrates the failure of the mist flow assumption is the condenser in a steam cycle, in which a liquid water film forms around cooling tubes and the vapor flow is 30 to 40 m/s [18]. Large pockets

of liquid water around the cooling tubes move much slower than the vapor, and it is only at the liquid-vapor interface where water droplets are under $1 \mu m$ in size and can be separated from the surface.

We now address the question of whether or not the mist flow assumption is reasonable in the context of a multiphase flow model of a PEM fuel cell. In the gas delivery channels, where the gas velocity can be as large as a few meters per second, the mist flow assumption may be applied if the size of liquid pockets is on the order of a few microns. However, the situation in the porous electrodes is very different since the gas flow velocities are much smaller. Simulations of flow in the gas diffusion layer of the PEMFC have demonstrated that conventional flow fields exhibit a gas velocity on the order of 0.01 cm/s, while for interdigitated flow fields the velocity can be as large as 5 cm/s [9, 10]. Considering that liquid droplets within the electrodes can be much larger than a micron in size, the liquid has too much inertia to be entrained by the impinging gas flow even when the gas velocity is as high as 5 cm/s in the interdigitated case.

4 Concluding Remarks

We have shown in this paper, using order of magnitude estimates of the equations governing multiphase condensing mixtures, that the liquid saturation depends strongly on the slip velocity between the liquid and gas phases. For mist models in which the liquid phase is assumed to be dispersed as small droplets within the gas phase, the slip velocity is zero and we argue that the saturation is consequently on the order of 10^{-4} . For multiphase flows, in which the liquid velocity is typically determined using Darcy's law along with some other physical assumption on liquid dynamics (such as when capillary pressure is the driving force), the saturation should be several orders of magnitude larger. We use several examples from the current fuel cell literature to illustrate this discrepancy and confirm our estimates. This is the first time that the connection between slip velocity and saturation in condensing mixtures has been explicitly addressed in the context of fuel cells.

The gas mixture velocities generated within the porous electrodes of a PEMFC appear to be insufficient to suspend liquid droplets within the gas stream. Consequently, the mist flow assumption must be critically examined in the context of fuel cells.

Acknowledgments

Financial support from the Renewable Energy Organization of Iran (SANA), the Natural Sciences and Engineering Research Council of Canada (NSERC), and the MITACS Network of Centres of Excellence is gratefully acknowledged.

References

- [1] Bakhtar, F., Mahpeykar, M. R. and Abbas, K. K. (1995) An investigation of nucleating flows of steam in a cascade of turbine blading – Theoretical treatment, *ASME Journal of Fluids Engineering*, 117:138–144.

- [2] Bakhtar, F. and Mohammadi Tochai, M. T. (1980) An investigation of two-dimensional flows of nucleating and wet steam by the time-marching method, *International Journal of Heat and Fluid Flow*, 2(1):5–18.
- [3] Berning, T. and Djilali, N. (2003) A 3D multiphase, multicomponent model of the cathode and anode of a PEM fuel cell, *Journal of the Electrochemical Society*, 150(12):A1598–A1607.
- [4] Bradean, R., Promislow, K. and Wetton, B. (2004) Phase change and two phase flow in cathode porous electrodes of fuel cells, Paper #IMECE2004-61347, in *Proceedings of the ASME International Mechanical Engineering Congress and Exposition*, Anaheim, CA, November 13–19.
- [5] Costamagna, P. (2001) Transport phenomena in polymeric membrane fuel cells, *Chemical Engineering Science*, 56:323–332.
- [6] Gerber, A. G. (2003) Two-phase Lagrangian/Eulerian model for nucleating steam flow, *ASME Journal of Fluid Engineering*, 124(2):465–475.
- [7] Gerber, A. G. and Kermani, M. J. (2004) A Pressure Based Eulerian-Eulerian Multiphase Model for Condensation in Transonic Steam Flows, *International Journal of Heat and Mass Transfer*, 47:2217–2231.
- [8] Gurau, V., Liu, H. and Kakaç, S. (1998) Two-dimensional model for proton exchange membrane fuel cells, *AIChE Journal*, 44(11):2410–2422.
- [9] He, W., Yi, J. S. and Nguyen, T. V. (2000) Two-phase Flow model of the cathode of PEM fuel cells using interdigitated flow fields, *AIChE Journal*, 46(10):2053–2064.
- [10] Hu, G. et al. (2004) Three-dimensional numerical analysis of proton exchange membrane fuel cells (PEMFCs) with conventional and interdigitated flow fields, *Journal of Power Sources*, 136:1–9.
- [11] Incropera, F. P. and DeWitt, D. P. (2002) *Fundamentals of Heat and Mass Transfer*, Fifth edition, John Wiley & Sons.
- [12] Kermani, M. J. and Stockie, J. M. (2004) Heat and Mass Transfer Modeling of Dry Gases in the Cathode of PEM Fuel Cells, *International Journal of Computational Fluid Dynamics*, 18(2):153–164.
- [13] Kermani, M. J., Stockie, J. M. and Gerber, A. G. (2003) Condensation in the Cathode of a PEM Fuel Cell, *Proceedings of the 11th Annual Conference of the CFD Society of Canada*, Vancouver, BC, Canada, May 28–30.
- [14] Kermani, M. J. and Gerber, A. G. (2003) A General Formula for the Evaluation of Thermodynamic and Aerodynamic Losses in Nucleating Steam Flow, *International Journal of Heat and Mass Transfer*, 46:3265–3278.
- [15] Khakbaz Baboli, M. and Kermani, M. J. (2008) A Two Dimensional, Transient, Compressible Isothermal and Two-Phase Model for the Air-Side Electrode of PEM Fuel Cells, *Electrochimica Acta*, 53 (26):7644–7654.

- [16] Khajeh-Hosseini-Dalasm, N., Fushinobu, K. and Okazaki, K. (2010) Three-Dimensional Transient Two-Phase Study of the Cathode Side of PEM Fuel Cell, *International Journal of Hydrogen Energy* 35:4234–4246.
- [17] Moran, M. J. and Shapiro, H. N. (1996) Fundamentals of Engineering Thermodynamics, Third edition, John Wiley & Sons.
- [18] Nag, P. (2001) Power Plant Engineering, Tata McGraw-Hill.
- [19] Natarajan, D. and Nguyen, T. V. (2001) A Two-Dimensional, Two-Phase, Multicomponent, Transient Model for the Cathode of a Proton Exchange Membrane Fuel Cell Using Conventional Gas Distributors, *Journal of the Electrochemical Society*, 148(12):A1324–A1335.
- [20] Nguyen, T. V. and White, R. E. (1993) A water and heat management model for proton-exchange-membrane fuel cells, *Journal of the Electrochemical Society*, 140(8):2178–2186.
- [21] Schack, A., Goldschmidt, H. and Partridge, E. P. (1966), Industrial Heat Transfer, John Wiley & Sons.
- [22] Shimpalee, S., Greenway, S., Spuckler, D. and Van Zee, J. W. (2004) Predicting water and current distributions in a commercial-size PEMFC, *Journal of Power Sources*, 135:79–87.
- [23] Um, S. and Wang, C. Y. (2004) Three-dimensional analysis of transport and electrochemical reactions in polymer electrolyte fuel cells, *Journal of Power Sources*, 125:40–51.
- [24] Wang, Z. H., Wang, C. Y. and Chen, K. S. (2001) Two-phase flow and transport in the air cathode of proton exchange membrane fuel cells, *Journal of Power Sources*, 94(1):40–50.
- [25] Weber, A. Z. and Newman, J. (2004) Modeling transport in polymer-electrolyte fuel cells. *Chemical Reviews*, 104(10):4679-4726.
- [26] White, A. J. and Young, J. B. (1993) Time-marching method for the prediction of two-dimensional, unsteady flows of condensing steam, *Journal of Propulsion and Power*, 9(4):579–587.